JOURNAL OF AEROSPACE COMPUTING, INFORMATION, AND COMMUNICATION
Vol. 1, December 2004

An Adaptive Vision-Based Approach to Decentralized Formation Control

Ramachandra Sattigeri [*] and Anthony J. Calise[†]
Georgia Institute of Technology, Atlanta, Georgia 30332-0150

and
Johnny H. Evers [‡]
Air Force Research Laboratory, Eglin Air Force Base, Florida 32542-6810

In considering the problem of formation control in the deployment of intelligent munitions, it would be highly desirable, both from a mission and a cost perspective, to limit the information that is transmitted between vehicles in formation. We have proposed an adaptive output feedback approach to address this problem. Adaptive formation controllers are designed that allow each vehicle in formation to maintain separation and relative orientation with respect to neighboring vehicles, while avoiding obstacles. We have implemented two approaches for formation control, namely, leader-follower formations and leaderless formations. In leader-follower formations, there is a unique leader and all the other vehicles are followers. In leaderless formations, there is no unique leader. Each vehicle tracks line-of-sight range to up to two nearest vehicles while simultaneously navigating towards a common set of waypoints. As our results show, such leaderless formations can perform maneuvers like splitting to go around obstacles, rejoining after negotiating the obstacles, and changing into line-shaped formation in order to move through narrow corridors.

Nomenclature

UAV	=	unmanned aerial vehicle
MAV	=	micro autonomous vehicle
LOS	=	line-of-sight
NN	=	neural network
MIMO	=	multi-input multi-output
DOF	=	degree of freedom
PCH	=	Pseudo-Control Hedging
SHL	=	Single Hidden Layer
IMU	=	Inertial Measuring Unit
LDC	=	Linear Dynamic Compensator
WP	=	Waypoint
NV	=	Number of Vehicles Tracked
cmd	=	command
com	=	command
rm	=	reference model

This paper is part of the December Special Section on Intelligent Systems. Received 19 August 2004; revision received 20 October 2004; accepted for publication 22 October 2004.

[*]Graduate Research Assistant, School of Aerospace Engineering, gte334x@prism.gatech.edu. AIAA Member
[†]Professor, School of Aerospace Engineering, anthony.calise@ae.gatech.edu. Fellow AIAA.
[‡]Chief, Autonomous Control Team, Munitions Directorate, evers@eglin.af.mil. Senior Member AIAA.

foll	=	follower
lead	=	leader
nom	=	nominal
FC	=	formation control
OA	=	obstacle avoidance
w.r.t.	=	with respect to
x	=	state vector of dimension n
y	=	output vector of dimension m
u	=	control vector of dimension m
$f(x,u)$	=	partially known system dynamics function
$g(x)$	=	partially known output vector function
r_i	=	relative degree of the i^{th} output y_i
r	=	vector relative degree
χ	=	state vector of the internal dynamics
ξ_i	=	vector of the i^{th} output y_i and its derivatives up to order $(r_i - 1)$
ξ	=	vector of all ξ_i, $i = 1,2,\ldots m$
$h_i(\xi,\chi,u)$	=	r_i^{th} time derivative of the i^{th} output y_i
$h(x,u)$	=	vector of all $h_i(\xi,\chi,u)$, of dimension m
t	=	time
y_{ci}	=	smooth, bounded reference trajectory for the i^{th} output y_i to track
$y_{ci}^{r_i}$	=	r_i^{th} time derivative of reference trajectory $y_{ci}(t)$
y_c^r	=	m dimensional vector of all $y_{ci}^{r_i}$, $i = 1,2,\ldots m$
ν	=	pseudo-control function
$\hat{h}_i(y,u)$	=	smooth invertible function
$\hat{h}(y,u)$	=	vector of all $\hat{h}_i(y,u)$, of dimension m
$\Delta(\xi,\chi,u)$	=	inversion error vector of dimension m
η	=	states of linear, dynamic compensator
ν_{dc}	=	linear, dynamic compensator output
ν_{ad}	=	NN output
u_{cmd}	=	commanded control (actuator) input
$\hat{u}$	=	estimate of control (actuator) output
u	=	actual control (actuator) output
$\tilde{y}_i$	=	output tracking error equal to $y_{ci} - y_i$
$\tilde{y}$	=	vector of tracking errors $\tilde{y}_i$, $i = 1,2,\ldots m$
E	=	error vector of $\tilde{y}_i$ and its time derivatives up to order $(r_i - 1)$, $i = 1,2,\ldots m$ and LDC states η
$\overline{A}$	=	stable error dynamics matrix
$\overline{B}$	=	input matrix for error dynamics
$\overline{\nu}_d(t)$	=	vector of delayed values of the pseudo-control vector v
$\overline{y}_d(t)$	=	vector of delayed values of the output vector y
$\overline{x}(t)$	=	input vector to NN
σ	=	squashing function
W	=	output layer weight matrix of SHL NN
V	=	input layer weight matrix of SHL NN
Γ_V	=	learning rate for SHL NN input layer weight matrix V

Γ_W = learning rate for SHL NN output layer weight matrix W
$\hat{E}$ = estimates of error vector E
P = positive-definite matrix solution of Lyapunov equation
Q = positive-definite matrix
λ_V = sigma-mod parameter for input layer weight matrix V
λ_W = sigma-mod parameter for output layer weight matrix W
ν_h = PCH signal
(x_i, y_i) = non-dimensionalized inertial position coordinates of the i^{th} aircraft
V_i = non-dimensionalized speed of the i^{th} aircraft
ψ_i = heading of the i^{th} aircraft, measured counterclockwise from inertial X axis
a_{i1} = non-dimensionalized lateral acceleration of the i^{th} aircraft
a_{i2} = non-dimensionalized longitudinal acceleration of the i^{th} aircraft
k_{i1}, k_{i2} = non-dimensionalized constants representing effect of drag on the i^{th} aircraft
R_{ij} = non-dimensionalized range between i^{th} and j^{th} aircraft
λ_{ij} = LOS angle of j^{th} aircraft w.r.t. i^{th} aircraft, measured counterclockwise from inertial X axis
$\hat{\lambda}_{ij}$ = unit vector aligned along the LOS direction from the i^{th} to the j^{th} aircraft
R_{com}^{ij} = non-dimensionalized range command between i^{th} and j^{th} aircraft
e_{ij} = error in commanded range, $e_{ij} = R_{com}^{ij} - R_{ij}$
p = time-constant of first order reference model for filtering range command
k_p = proportional control gain
$R_{c(i,j)}$ = non-dimensionalized reference range command between i^{th} and j^{th} aircraft
$\hat{I}, \hat{J}$ = unit vectors aligned along the inertial X and Y axes respectively
$\alpha_{(i,j)}$ = estimate of the achieved pseudo-control for aircraft i along the direction $\hat{\lambda}_{ij}$
$\Delta_{(i,j)}$ = inversion error of aircraft i corresponding to the approximate inversion of $\dot{R}_{ij}$
c_1 = real number lying between 0 and 1
(x_{WP}, y_{WP}) = non-dimensionalized inertial waypoint coordinates
R_1 = non-dimensionalized range to closest aircraft
R_2 = non-dimensionalized range to second closest aircraft
$R_{\max 1}, R_{\max 2}$ = non-dimensionalized positive range constants
λ_1 = LOS angle to closest aircraft
λ_2 = LOS angle to second closest aircraft
$\hat{\lambda}_1, \hat{\lambda}_2$ = unit vector aligned along λ_1 and λ_2 respectively
$\langle \bullet \rangle$ = dot product operator
$sat(\cdot)$ = linear saturation operator

I. Introduction

As demonstrated in recent conflicts, UAVs are becoming an important component of our military force structure. UAVs, operating in close proximity to enemy forces, provide real-time information difficult to obtain from other sources, without risk to human pilots. Among the weapons employed by these UAVs will be flocks of cooperative MAVs operating in close proximity to terrain or structures that will gather information on enemy

movements and, under human supervision, seek out, identify, and attack targets of opportunity. In large groups of MAVs or small UAVs, even small percentage reductions in drag will offer significant increased payoffs in the ability to maintain persistent coverage of a large area. One concept, well known to bicyclists, race car drivers, and pilots and exploited by swimming and flying animals, is the benefit of operating in the wake of another vehicle (or organism). Therefore maintaining a formation while at the same time executing searches in a congested environment will be a primary requirement. Stealth like operations will also be important, implying the need to maintain autonomy and to minimize communication. Maintaining a formation is also important from this perspective so that passive (vision based) sensing can be used to ascertain the locations and behaviors of cooperating MAVs/UAVs.

Standard approaches for formation control include the leader-follower, behavior-based and the virtual structure approaches. In leader-follower based approach,[1,2] one vehicle is designated as a leader and the remaining vehicles as followers. The followers track the range from the leader and other followers to desired values. The leader sets a nominal trajectory for the formation to follow and may cooperate with the followers in regulating range. In the virtual structure approach, the entire formation is treated as a single entity.[3,4] Desired motion is assigned to this single entity, the virtual structure, which traces out trajectories for each member in the formation to track. In behavior-based approaches,[5,6] several desired behaviors are prescribed for each vehicle and the final control is derived from a weighting of the relative importance of each behavior. Since in the leader-follower and virtual structure based approaches, coordination is with respect to a central agent, the formation controls lack robustness. Behavior-based approaches are decentralized and are significantly easier to implement. However, these are difficult to analyze mathematically and formation convergence to desired configurations is not guaranteed.

Although imperfectly understood, flocking behavior of birds, schooling behavior of fish, and even studies of swarming insects have provided inspiration for concepts of coordinated multi-vehicle operation.[7] Reynolds[8] introduced a model that suggests flocking is the combined result of three simple steering rules that each agent follows independently. In this model, each agent can access the whole scene's geometric description, but flocking requires that it react *only* to flock-mates within a certain small neighborhood. Reynolds rules were validated in a graph-theoretic and Lyapunov stability analysis framework.[9,10] Convergence properties on individual agent velocity vectors and relative distances were shown. Reference 10 also provided a framework for addressing splitting, rejoining and squeezing maneuvers for flocks in the presence of multiple obstacles.

In our approach, we assume that the vehicles do not communicate velocity vector information. The lack of relative velocity vector information is treated as modeling uncertainty, whose effect on LOS range (output) regulation is to be canceled by the output of an online adaptive NN.[2] As a result, each vehicle can regulate both the range and relative orientation to a leader and/or neighboring vehicle without knowing the state and control policy of that vehicle. It is assumed that each vehicle can measure its own speed, heading, range and angle to other vehicles. The theory is based on an error observer approach to adaptive output feedback control of uncertain, MIMO systems.[11] The approach is adaptive to both parametric uncertainty and unmodeled dynamics. The method of Pseudo-Control Hedging (PCH) [12,13] is used to protect the adaptive process from actuator limits and actuator dynamics. It is also used to protect the adaptive process during periods when it is not in control of the vehicle.

Because of the robustness issues associated with leader-follower formations, we propose a coordination scheme that does not depend on a *unique* leader. In this scheme, which we call a leaderless formation scheme, each vehicle tracks LOS range to up to two nearest vehicles while simultaneously navigating towards a common set of waypoints. For a vehicle to be tracked, it must lie within a specified range from another vehicle. The leaderless nature of this scheme renders the formation robust to failures in one or more vehicles. Changes in the formation shape required while negotiating different obstacles are easier to implement using this approach. Since the number of vehicles that can be tracked using this approach is 0, 1, or 2, the control laws may be switching. Switching of the control laws can lead to the adaptive controller associated with tracking a particular neighboring vehicle to not be in control of the plant. In such cases, PCH is vital to the stability of the adaptation process.[18]

The contribution of this paper is to propose a vision-based, adaptive framework for the formation control of multiple vehicles, with minimal information communication between the vehicles. Vision-based sensors onboard each vehicle are employed to provide estimates of relative LOS range and angle w.r.t. neighboring vehicles. Adaptive NNs in each vehicle are trained online with a combination of vision-based measurements and measurements from IMUs to estimate velocity relative to the neighboring vehicles. These estimates are required in the guidance policy for each vehicle. This framework provides a novel application of vision-in-the-loop control.

The organization of the paper is as follows. The next section summarizes the theory for the error observer approach and states the problem formulation for decentralized formation control. Next, we review the inverting control design for formation control. We also briefly discuss the static obstacle avoidance controller. Simulation results for a leader-follower team of 4 members regulating LOS range from each other are shown. Following this,

the coordination scheme for *leaderless* formation flying is described. Simulation results with this scheme are shown for a team of 5 members. The results show splitting, rejoining and squeezing maneuvers in the presence of obstacles.

II. Adaptive Output Feedback Approach

Consider the observable nonlinear system described by

$$\begin{aligned} \dot{x} &= f(x,u) \\ y &= g(x) \end{aligned} \tag{1}$$

where $x \in \Omega \subset \Re^n$ are the states of the system, $u, y \in \Re^m$ are the controls and regulated output variables respectively, and $f(\cdot,\cdot), g(\cdot)$ are uncertain functions. Moreover n need not be known.

A. Assumption

The system in Eq. (1) satisfies the condition for output feedback linearizability with vector relative degree $[r_1, r_2, \ldots, r_m]^T$, $r = r_1 + r_2 + \ldots r_m \le n$.[14]

Then there exists a mapping that transforms the system into the so-called normal form:

$$\begin{aligned} \dot{\chi} &= f'(\xi, \chi) \\ \dot{\xi}_i^1 &= \xi_i^2 \\ &\vdots \\ \dot{\xi}_i^{r_i} &= h_i(\xi, \chi, u) \\ \xi_i^1 &= y_i, \; i = 1,2,\ldots,m, \end{aligned} \tag{2}$$

where $h_i(\xi, \chi, u) = h_i(x,u)$, where $\xi = \left[\xi_1^T \; \ldots \; \xi_m^T\right]^T$, $\xi_i = \left[\xi_i^1 \; \ldots \; \xi_i^{r_i}\right]^T$ and χ are the states associated with the internal dynamics. Note that ξ_i^{j+1} is simply the j^{th} time derivative of y_i .

B. Assumption

The zero dynamics are asymptotically stable.

The objective is to design an output feedback control law that causes $y_i(t)$ to track a smooth bounded reference trajectory $y_{ci}(t)$ with bounded tracking error.

C. Controller Design and Tracking Error Dynamics

Feedback linearization is achieved by introducing the following inverse

$$u = \hat{h}^{-1}(y, \nu) \tag{3}$$

where

$$\nu = \hat{h}(y,u) \tag{4}$$

is the pseudo-control signal. The pseudo-control signal $\hat{h}(y,u)=\left[\hat{h}_1(y,u),\ldots,\hat{h}_m(y,u)\right]^T$ represents an invertible approximation to $h(x,u)=\left[h_1(x,u),\ldots,h_m(x,u)\right]^T$ in Eq. (2), which is limited to using only the available measurements and control signal. If outputs other than the regulated output are available for feedback, they may also be used in Eq. (3) to form the approximate inverse.

Thus the system dynamics, as far as the regulated output variable is concerned, is given by,

$$y^r = \nu + \Delta \tag{5}$$

where

$$\Delta(\xi,\chi,\nu) = h\left(\xi,\chi,\hat{h}^{-1}(y,\nu)\right) - \hat{h}\left(y,\hat{h}^{-1}(y,\nu)\right) \tag{6}$$

is the inversion error that results from the use of Eq. (3) in place of an exact state feedback inverse. The pseudo-control is chosen to have the form

$$\nu = y_c^r + \nu_{dc} - \nu_{ad} \tag{7}$$

where y_c^r are generated by stable reference models that define the desired closed-loop behavior, ν_{dc} is the output of a dynamic compensator designed to stabilize the linearized error dynamics, and ν_{ad} is the adaptive component.

From Eq. (5) and Eq. (7), the error dynamics are given as,

$$\tilde{y}^r = y_c^r - y^r = -\nu_{dc} + \nu_{ad} - \Delta(x,\nu) \tag{8}$$

From Eq. (6) and Eq. (7) it is seen that Δ depends on ν_{ad} through ν, and Eq. (8) shows that ν_{ad} has to be designed to cancel Δ. Therefore the following assumption is introduced to guarantee existence and uniqueness of a solution for ν_{ad}.

D. Assumption

The map $\nu_{ad} \mapsto \Delta$ is a contraction over the entire input domain of interest. It can be shown that this assumption leads to the following conditions[15]

$$\text{i) } \operatorname{sgn}\left(\frac{\partial h_i}{\partial u_i}\right) = \operatorname{sgn}\left(\frac{\partial \hat{h}_i}{\partial u_i}\right),\ i = 1,2,\ldots,m$$

$$\text{ii) } \left|\frac{\partial \hat{h}_i}{\partial u_i}\right| > \frac{1}{2}\left|\frac{\partial h_i}{\partial u_i}\right| > 0,\ i = 1,2,\ldots,m$$

The first condition requires that the sign of the control effectiveness is modeled correctly and the second places a lower bound on the estimate of the control effectiveness.

E. Error Observer

It can be shown that the error dynamics in Eq. (8) can be written as

$$\dot{E} = \overline{A}E + \overline{B}\left[\nu_{ad} - \Delta\right] \tag{9}$$

where the elements of E are made up of $\tilde{y}_i$ and its derivatives up to order $(r_i - 1)$ and the dynamic compensator states. An error observer is designed based on this equation,[11] which results in error estimates $\hat{E}$ that are used in the adaptive update law given below.

F. Approximation of the Inversion Error

The inversion error Δ can be approximated to any desired degree of accuracy by using a Single Hidden Layer Neural Network (SHL NN) with sufficient number of hidden layer neurons, and having the following input vector,[16,17]

$$\bar{x}(t) = \left[1 \;\; \bar{v}_d^T(t) \;\; \bar{y}_d^T(t)\right]^T \tag{10}$$

where

$$\bar{v}_d^T(t) = \left[\nu(t), \nu(t-d), \ldots, \nu\left(t-(n_1-1)d\right)\right]^T,$$

$$\bar{y}_d^T(t) = \left[y(t), y(t-d), \ldots, y\left(t-(n_1-1)d\right)\right]^T$$

with $n_1 \geq n$. Since n is unknown, a sufficient number of delayed signals are required. The input-output map of a SHL NN is given by

$$\nu_{ad} = W^T \sigma\left(V^T \bar{x}\right) \tag{11}$$

where σ is the so-called squashing function. The NN is trained online with the adaptive law

$$\begin{aligned} \dot{W} &= -\Gamma_W \left[2\left(\sigma\left(V^T\bar{x}\right) - \sigma'\left(V^T\bar{x}\right)V^T\bar{x}\right)\hat{E}^T P\overline{B} + \lambda_W W\right] \\ \dot{V} &= -\Gamma_V \left[2\bar{x}\hat{E}^T P\overline{B}W^T\sigma'\left(V^T\bar{x}\right) + \lambda_V V\right] \end{aligned} \tag{12}$$

where $\sigma'(z) = \text{diag}\left(\frac{d\sigma_i}{dz_i}\right)$, P is the positive definite solution to the Lyapunov equation $\bar{A}^T P + P\bar{A} + Q = 0$, with Q>0, and Γ_W and Γ_V are the adaptation gains. It has been shown that the adaptive law in Eq. (12) guarantees (subject to upper and lower bounds on the adaptation gains) that all error signals and the NN weights are uniformly ultimately bounded.[11]

G. Pseudo-Control Hedging (PCH)

PCH is introduced to protect the adaptive law from effects due to actuator rate and position limits, unmodeled actuator dynamics and to protect the adaptive process when it is not in control of the plant.[12,13] The main idea behind PCH methodology is to modify the reference command, y_c, in order to prevent the adaptive element from adapting to these actuator characteristics. This is commonly done by generating the command using a reference model for the desired response. The reference model is 'hedged' by an amount equal to the difference between the commanded and an estimate for the achieved pseudo-control. To compute this difference, a measurement or estimate of the actuator position $\hat{u}$ is required. The pseudo-control hedge signal is given by,

$$\nu_{h_i} = \hat{h}_i\left(y, u_{cmd_i}\right) - \hat{h}_i\left(y, \hat{u}_i\right),\ i = 1,2,\ldots,m\ . \tag{13}$$

where y_{cmd_i} is the external command signal, then the reference model update *with PCH* is set to

$$y_{c_i}^{r_i} = h_{rm_i}\left(y_{c_i}, \dot{y}_{c_i}, \ldots, y_{c_i}^{r_i-1}, y_{cmd_i}\right) - \nu_{h_i} \tag{14}$$

The instantaneous output of the reference model used to construct the pseudo-control signal remains unchanged and is given by

$$\nu_{rm_i} = h_{rm_i}\left(y_{c_i}, \dot{y}_{c_i}, \ldots, y_{c_i}^{r_i-1}, y_{cmd_i}\right) \tag{15}$$

The block diagram of the MRAC controller architecture with PCH and error observer is given below.

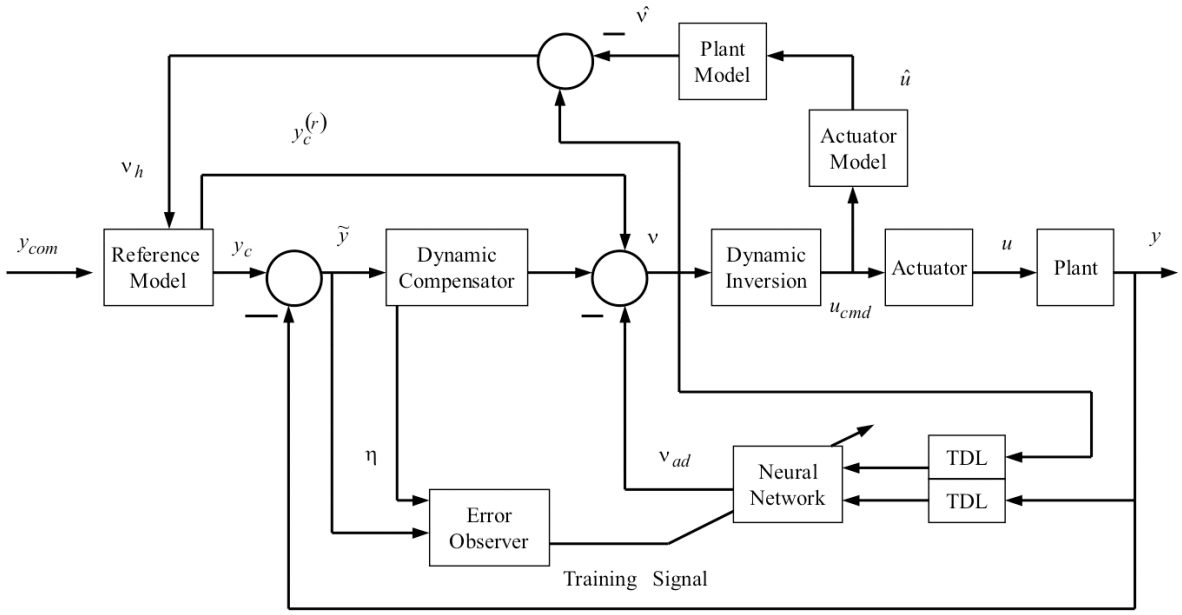

Fig. 1 MRAC Architecture with PCH.

III. Formation Control Formulation

Consider a group of N vehicles whose individual dynamics are given by,

$$\dot{x}_i = f_i(x_i, u_i),\ i = 1,2,\ldots,N \tag{16}$$

where x_i represents the states and u_i the control vector of the i^{th} vehicle. Assume that vehicles i and j cooperate by regulating a *joint* variable (e.g., LOS range)

$$z = g(x_i, x_j) \tag{17}$$

whose relative degree (r) is known, so that,

$$z^{(r)} = g_r(x_i, x_j, u_i, u_j) \tag{18}$$

To arrive at a decentralized control solution, the following approximation is employed by the i^{th} vehicle

$$z_i^{(r)} = \hat{g}_{ri}(z, x_i, u_i) = \nu_i \tag{19}$$

Equation (19) forms the basis for an inverting control design in which the inversion error is

$$\Delta_i = g_r\left(x_i, x_{j,} u_i, u_j\right) - \hat{g}_{ri}\left(z, x_i, u_i\right) \tag{20}$$

Vehicle $i^{'}s$ inverting solution is augmented with a NN that estimates and approximately cancels Δ_i. The input vector to the NN for the i^{th} vehicle is given by $\mu_i = \left[x_i, \bar{u}_{id}(t), \bar{z}_d(t)\right]^T$, where $\bar{u}_{id}(t), \bar{z}_d(t)$ are vectors of sufficiently large number of delayed values of $u_i(t), z(t)$ respectively.[16,17] So, the decentralized control solution of all cooperating aircraft is given by $u_i = \hat{g}_{ri}^{-1}\left(\nu_i, z, x_i\right)$, where ν_i is constructed as in Eq. (7).

IV. Application to Formation Control

The formation of vehicles is constrained to lie in a two-dimensional plane. The vehicles are considered to be point-mass objects that can accelerate both along and perpendicular to the direction of motion. The non-dimensionalized equations of motion for the i^{th} aircraft are given by [2]

$$\dot{x}_i = V_i \cos\psi_i \tag{21}$$

$$\dot{y}_i = V_i \sin\psi_i \tag{22}$$

$$\dot{\psi}_i = \frac{a_{i1}}{V_i} \tag{23}$$

$$\dot{V}_i = a_{i2} - k_{i1}V_i^2 - k_{i2}\left(\frac{a_{i1}^2 + 1}{V_i^2}\right) \tag{24}$$

where $\left(x_i, y_i\right)$ are the inertial position coordinates, ψ_i, V_i are the heading and speed variables, k_{i1}, k_{i2} are constants representing the effect of drag forces and a_{i1}, a_{i2} are the controls representing non-dimensionalized acceleration. Bounds are placed on the controls to prevent slowing below the stall speed, and to prevent exceeding maximum bank angle limits and maximum and minimum longitudinal acceleration limits.[2] We model the actuator system as a saturation element with limits described above

$$u = \text{sat}\left(u_{cmd}\right) \tag{25}$$

Figure 2 shows the variables involved in describing the LOS kinematics. The LOS kinematics of the i^{th} aircraft with respect to the j^{th} aircraft is given by

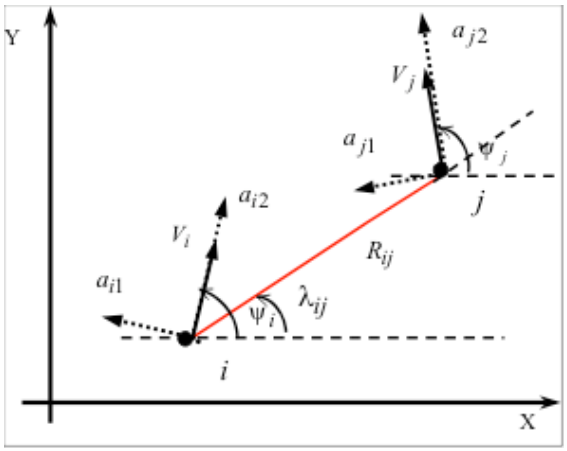

Fig. 2 LOS kinematics.

$$\dot{R}_{ij} = V_j \cos\left(\psi_j - \lambda_{ij}\right) - V_i \cos\left(\psi_i - \lambda_{ij}\right) \tag{26}$$

$$\dot{\lambda}_{ij} = \frac{V_j \sin\left(\psi_j - \lambda_{ij}\right) - V_i \sin\left(\psi_i - \lambda_{ij}\right)}{R_{ij}} \tag{27}$$

The information available to aircraft *i* include: V_i, ψ_i (by use of an IMU), R_{ij}, λ_{ij} (through vision-based sensors) and the control signals a_{i1}, a_{i2}.

A. Adaptive Formation Control Design

We design an inverting controller augmented with a NN for aircraft *i* for regulating the LOS range R_{ij} with respect to aircraft j. The controller architecture is as shown in Fig 1. The relative degree of R_{ij} with respect to the speed and heading of aircraft *i* is 1. Hence the range command R^{ij}_{com}, for the separation between the aircraft i and j, is filtered through a first order reference model. Figure 3 shows the hedged reference model. A rate limit is introduced so that the reference model does not command large range rates when the range error is large. The parameter p is the time constant and is a design parameter.

The dynamic compensator portion of the pseudo-control is a proportional error controller, $\nu_{dc(i,j)} = k_{p_i}\left(R_{c(i,j)} - R_{ij}\right)$. Referring to Eq. (7) the pseudo-control signal is

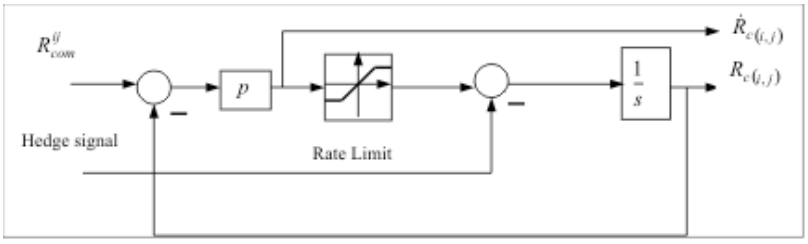

Fig. 3 Hedged reference model.

$$\nu_{(i,j)} = \dot{R}_{c(i,j)} + k_{p_i}\left(R_{c(i,j)} - R_{ij}\right) - \nu_{ad(i,j)} \tag{28}$$

The pseudo-control signal $\nu_{(i,j)}$ is the commanded LOS range-rate for aircraft i with respect to aircraft j. The pseudo-control signal is inverted to give a commanded velocity vector $\vec{V}_{FC_i}$. In case aircraft i is regulating LOS range with respect to multiple neighboring aircraft, say $m > 1$ in number, then the commanded velocity vector for aircraft i is given by the vector sum of the pseudo-control signals oriented along λ_{ij} [2]

$$\vec{V}_{FC_i} = -\sum_{j,j\neq i}^{m} \vec{\nu}_{(i,j)}, \tag{29}$$

$$\vec{\nu}_{(i,j)} = \nu_{(i,j)}\hat{\lambda}_{ij} = \nu_{(i,j)}\left(\cos\lambda_{ij}\hat{I} + \sin\lambda_{ij}\hat{J}\right) \tag{30}$$

where $\hat{\lambda}_{ij}$ is the unit vector along the LOS from aircraft i to aircraft j, and $\hat{I}, \hat{J}$ are unit vectors aligned along the X and Y inertial axes respectively.

B. Hedge Signals

Equations (29) and (30) show that when commanding range with respect to $m > 1$ aircraft, we are actually trying to track *m* pseudo-control signals with just one control variable, the velocity vector. This means each aircraft is an underactuated system when it commands range with respect to multiple aircraft. In this case, the method of calculating the hedge signal is special. We do a non-orthogonal projection of the actual velocity vector along each of the unit vector directions $\hat{\lambda}_{ij}$, $j = 1,\ldots m, j \neq i$. Each of these projections is treated as the achieved pseudo-control along the particular direction $\hat{\lambda}_{ij}$. The difference between the commanded pseudo-control and the achieved pseudo-control signal is the hedge signal. The actual mathematics for doing the above calculation is shown below.

$$\vec{V}_i = -\sum_{j,j\neq i}^{m} \alpha_{(i,j)}\hat{\lambda}_{ij} = -\overline{N}_i\left[\vec{\alpha}_i\right] \tag{31}$$

where the k^{th} column of $\overline{N}_i$ is $\hat{\lambda}_{ik}$ and $\left[\vec{\alpha}_i\right]$ is the vector of elements $\alpha_{(i,j)}$, for all j, $j \neq i$. Note that $\alpha_{(i,j)}$ is the estimate of the achieved pseudo-control for aircraft i along the direction $\hat{\lambda}_{ij}$.

Thus we can solve Eq. (31) to obtain

$$\left[\vec{\alpha}_i\right] = -\overline{N}_i^{-1}\vec{V}_i \tag{32}$$

The corresponding expression for the PCH signal then becomes

$$\nu_{h_{(i,j)}} = \nu_{(i,j)} - \alpha_{(i,j)} \tag{33}$$

The corresponding expression for inversion error $\Delta_{(i,j)}$ is given as

$$\Delta_{(i,j)} = \dot{R}_{ij} - \alpha_{(i,j)} \tag{34}$$

C. Static Obstacle Avoidance

To illustrate the concept, it is assumed that the obstacles are contained within bounding spheres (circles in 2 dimensions), and that the centers (X_o, Y_o) and radii (r) of the obstacles are known. The goal of this strategy is to keep an imaginary line L_o of length D_o, originating at the vehicle's current position and extending in the direction of the velocity vector, from intersecting with any obstacle boundary.* The length of this line is typically based upon the vehicle's speed and maneuverability. An obstacle further away than this length D_o is not an immediate threat. The obstacle avoidance behavior considers each obstacle in turn and determines if they intersect with L_o. The obstacle which intersects L_o nearest the aircraft is selected as the "most threatening" and corrective steering action is undertaken to avoid this obstacle. If no obstacle collision is imminent, no steering action is taken. Corrective steering action to avoid an obstacle involves a speed and heading change command. The heading change command $\Delta\psi_{OA_i}$ is towards the closest projected edge of the obstacle in the local velocity fixed frame as shown in Fig 4. The output of the static obstacle avoidance controller is the commanded velocity vector $\vec{V}_{OA}$. Please refer to Ref. [2] for details of constructing $\vec{V}_{OA}$.

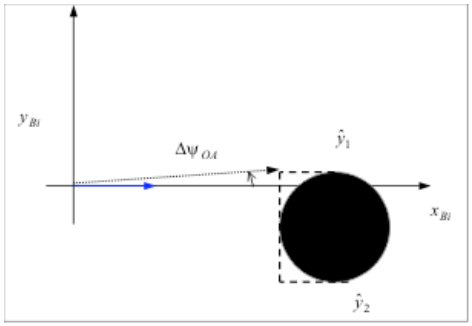

Fig. 4 Static obstacle avoidance.

D. Velocity Command Blending

The composite velocity vector command is given by blending the outputs of the formation controller and the obstacle avoidance controller. The velocity command for a follower vehicle is

$$\vec{V}_{cmd_{foll}} = c_1 \vec{V}_{OA_{foll}} + (1 - c_1)\vec{V}_{FC_{foll}} \tag{35}$$

The weight c_1, $0 \le c_1 \le 1$, is chosen such that obstacle avoidance has higher priority than formation control.[2] The velocity command for the leader vehicle is

* Craig Reynolds, "Not Bumping Into Things," Available online at http://www.red3d.com/cwr/nobump/nobump.html (cited Dec. 2004).

$$\vec{V}_{cmd_{lead}} = c_1 \vec{V}_{OA_{lead}} + k(1 - c_1)\vec{V}_{FC_{lead}} + (1 - c_1 - k(1 - c_1))\vec{V}_{nom} \tag{36}$$

where $\vec{V}_{nom}$ is a nominal velocity vector command for the leader. The leader aircraft would command $\vec{V}_{nom}$ if it were not avoiding obstacles and not regulating range from its followers. The factor k is set equal to 0.2 implying that formation control is the lowest priority for the leader.

Collisions between aircraft in close proximity can occur when one or more aircraft is only avoiding obstacles, i.e., $c_1 \approx 1$ in Eqs. (35) and (36). This is because Eqs. (35) and (36) do not include a command for collision avoidance that kicks in when the range between aircraft is dangerously low.

E. Inner-Loop Controller

The velocity vector command of Eqs. (35) and (36) is resolved into a speed command V_{cmd_i} and a heading command ψ_{cmd_i}, that are input to an inner-loop controller. The index i refers to both leader and follower aircraft. The inner-loop controller generates acceleration commands that depend on the speed and heading commands.

$$\begin{aligned} a_{i1cmd} &= \frac{1}{\tau_\psi}(\psi_{cmdi} - \psi_i)V_i \\ a_{i2cmd} &= \frac{1}{\tau_V}(sat[V_{cmdi}] - V_i) + k_{i1}V_i^2 + \frac{k_{i2}}{V_i^2}(a_{i1cmd}^2 + 1) \end{aligned} \tag{37}$$

where $\tau_V > 0$, $\tau_\psi > 0$ are the time constants of the inner-loop controller, and $sat(\cdot)$ is the linear saturation operator. V_{cmd_i} is limited to prevent saturating the actuators and to prevent speed commands lower than the stall speed.[2] The acceleration commands are limited in accordance with Eq. (25). Autopilot and throttle control lags are not modeled.

F. Simulation Results

We consider a team of 4 aircraft flying in formation. Aircraft 1 is the team leader. The nominal velocity vector command $\vec{V}_{nom}$ for the leader involves tracking a set of waypoints at constant speed. The nominal trajectory that results for the leader by commanding $\vec{V}_{nom}$ is shown in Fig. 5.

We specify a set of LOS range commands for all pairs of aircrafts in formation. Cooperation between the aircraft is imposed by having all aircraft regulate LOS range from each other. The aircrafts are referenced by the indices 1, 2, 3, 4. For the simulation, the following values of LOS ranges between pairs of aircraft were commanded:

$$\begin{aligned} R_{com}^{12} &= R_{com}^{13} = R_{com}^{24} = R_{com}^{34} = 1.0 \\ R_{com}^{14} &= R_{com}^{23} = \sqrt{2} \end{aligned}$$

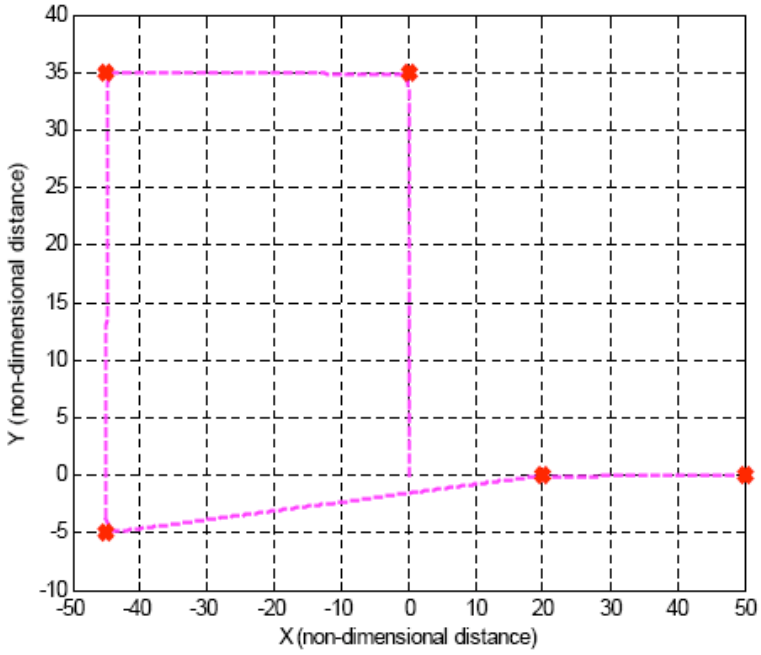

Fig. 5 Nominal leader trajectory.

We present results for cases with adaptation (NN on) and without adaptation (NN off). Hedging is on (H on) only for NN on. The hyperlinks multimedia 3 and 4 are movies that show the dynamic trajectory plot of the formation with the NN off and NN on respectively. In the top area of the movies, the global picture of how the formations evolve is shown while the bottom area shows the zoomed in formation. The objective of the movies is to show that adaptation enhances the cooperation between the aircraft in formation. This can be seen by noting how the aircraft transition into formation with NN off (multimedia 3) and NN on (multimedia 4) respectively. With the NN off, we see aircrafts 1 and 3 looping in circles before getting into formation. With the NN on, the transition into the formation is smooth. Secondly, with the NN off the errors in commanded range $\left(e_{ij} = R_{com}^{ij} - R_{ij}\right)$ are large in steady-state compared to that with the NN on. Figures 6 and 7 show these respective results.

It is also seen with NN on, the leader aircraft tracks more waypoints than with NN off in the same duration of time. This is because with the NN off, the leader slows down for the followers to catch up with it, and the formation flies at a lower speed in the steady state. We can thus infer that cooperation between the aircraft is enhanced with NN on. The speed histories for the formation with NN off and NN on are shown in Figs 8 and 9 respectively.

For the case with NN off (Figs. 6 and 8), the aircraft turn at the first two waypoints at approximately 50 and 110 seconds respectively. Note from the dynamic trajectory in multimedia 3 that the simulation stops when the formation is heading towards the 3rd waypoint. For the case with NN on (Figs. 7 and 9), the aircraft turn at the first 4 waypoints at approximately 30, 62, 90 and 135 seconds respectively.

Disturbances introduced at the control input (acceleration) level were found not to affect the formation trajectories and only caused increased oscillations and saturation in the controls. The performance of the NN in compensating for the inversion error was not affected.

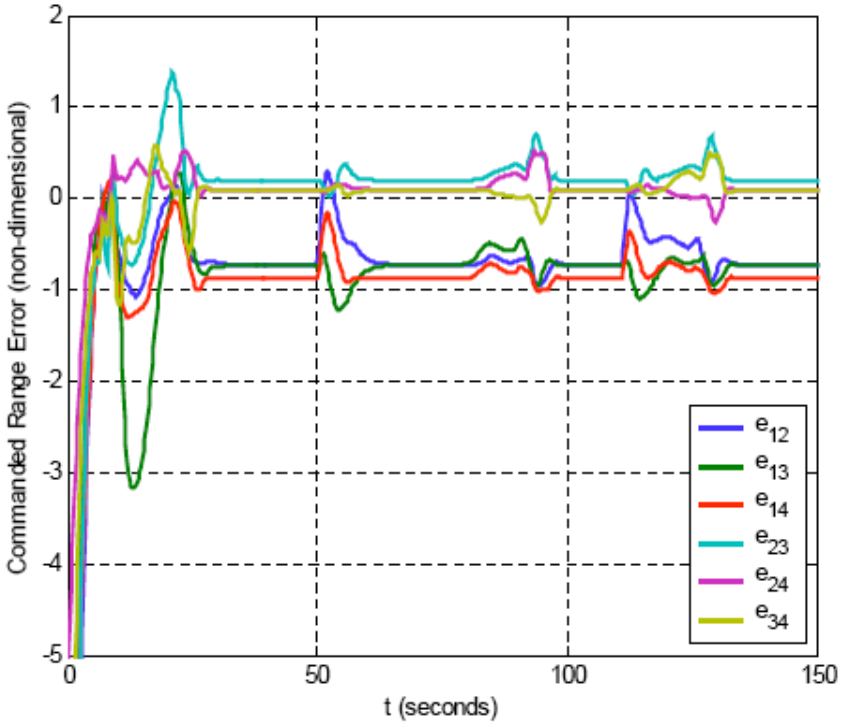

Fig. 6 Error in commanded range (NN off).

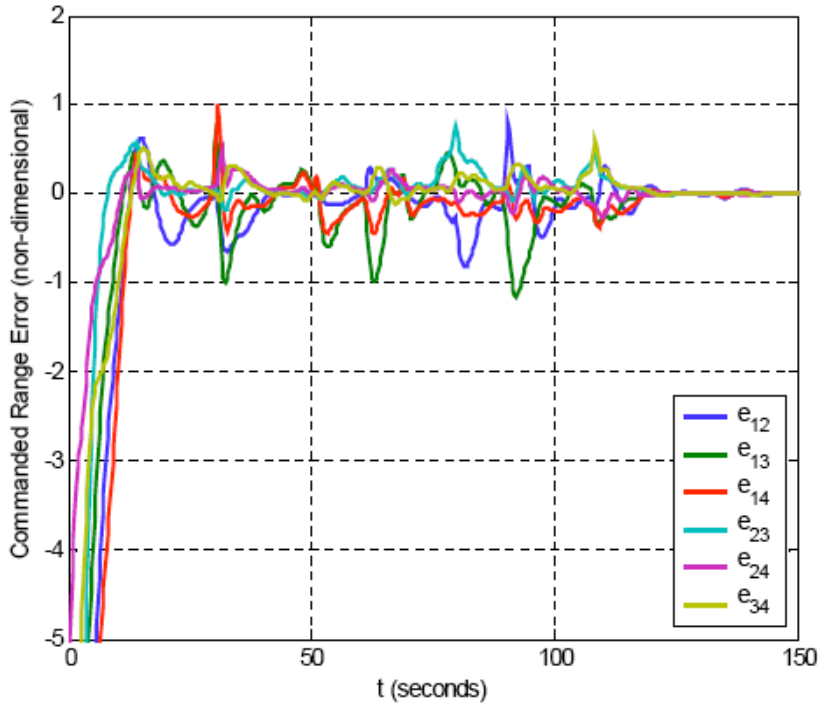

Fig. 7 Error in commanded range (NN on).

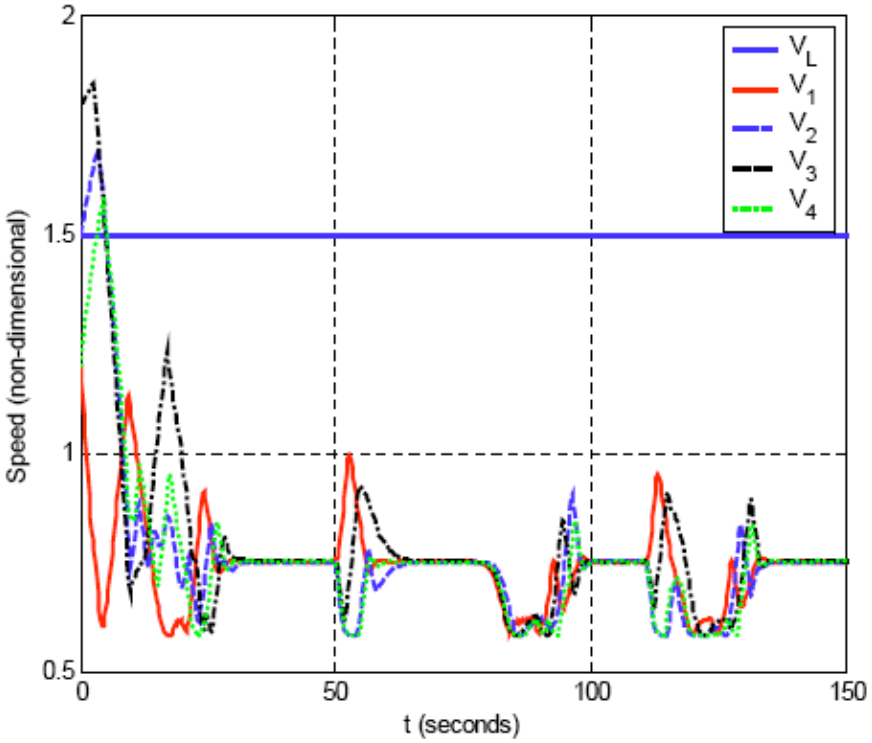

Fig. 8 Speed histories (NN off).

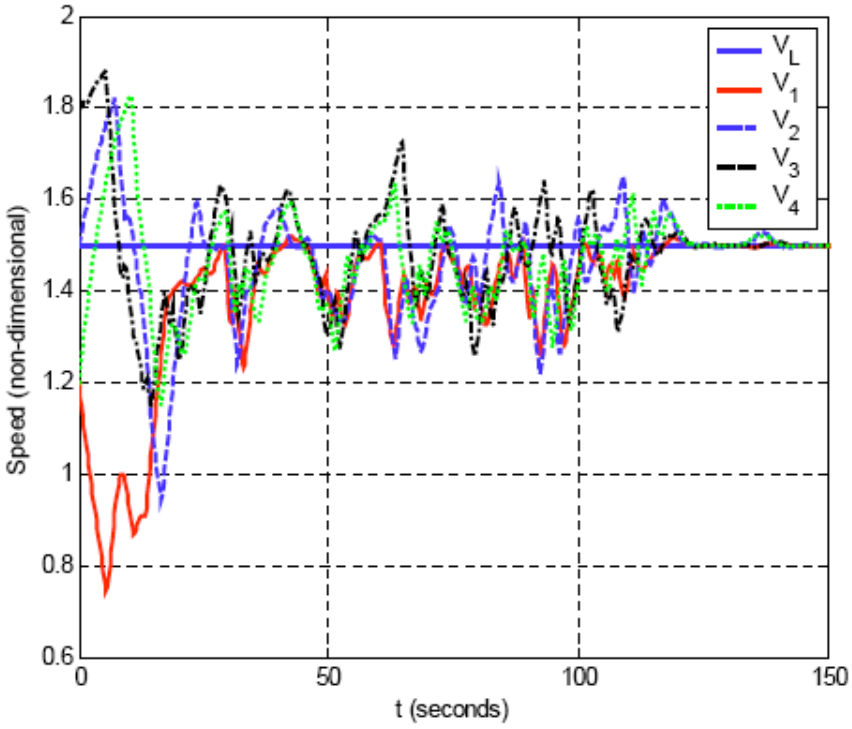

Fig. 9 Speed Histories (NN on).

V. Coordination Scheme for Leaderless Formation Flying

The problem with a leader-follower formation control scheme is in the concept of a designated leader. Such a formation lacks robustness to a failure in the leader vehicle. Secondly, it is not practical to pre-specify LOS ranges between pairs of vehicles for large numbers of vehicles in formation. Possibilities of failure in one or more follower vehicles further complicate this problem. So, we propose a coordination scheme that does not depend on a unique leader, is robust to failures in one or more vehicles and allows easy scaling of the formation.

We remove the assumption of a designated leader for the formation. Each vehicle now commands a nominal velocity vector when not tracking any neighboring vehicle. The nominal velocity involves heading towards a set of waypoints at constant speed. The set of waypoints is common to all the vehicles. The nominal velocity vector $\vec{V}_{nom}$ is given as

$$\begin{aligned} V_{nom_i} &= V_L \\ \psi_{nom_i} &= a\tan 2\left(y_{WP} - y_i, x_{WP} - x_i\right) \end{aligned} \tag{38}$$

where (x_{WP}, y_{WP}) represent inertial coordinates of the waypoints. Once the vehicle comes within a specified distance of one waypoint, it starts heading towards the next waypoint. The order in which the waypoints are tracked is the same for all vehicles.

Each vehicle tracks up to two nearest vehicles depending upon the range to the vehicle. The algorithm for choosing the number of vehicles to track is described in Fig. 10.

Let $R_1(t)$ and $R_2(t)$ denote LOS ranges to two nearest vehicles. Let $R_{\max} > 0$ be a constant and NV the number of vehicles tracked.

If $R_1(t) > R_{\max 1}$
$NV = 0$
Else if $R_2(t) \le R_{\max 2}$
$NV = 2$
Else
$NV = 1$
End

Fig. 10 Logic for choosing number of vehicles to track.

The formation control objective is to regulate range from NV number of nearest vehicles to R_{com}. The value for R_{com} is such that $0 < R_{com} < R_{\max 2} \le R_{\max 1}$ and is a constant for all the vehicles in the formation.

When the number of nearest neighbors NV changes, the control law switches. Switching of the control laws also takes place when a nearest neighbor is replaced.

We design adaptive formation controllers to regulate LOS range from every vehicle in the formation, but tracking takes place only with NV number of neighbors. This means that adaptation with respect to all the vehicles in the formation takes place all the time but not all of these adaptive controllers are in control of the plant, and switches can take place between the adaptive controllers that are in control of the plant. PCH allows adaptation to continue safely when not in control of the plant[18].

Switching between the adaptive controllers that are in control of the plant causes discontinuities in the commands that are input to the inner-loop controller [Eq. (37)]. But these discontinuities are not much of a problem if they do not occur rapidly, i.e., if the rate at which these discontinuities occur is significantly smaller than the bandwidth of the inner-loop controller. Rapid switching between the adaptive controllers that are in control of the plant can lead to oscillatory responses and poor performance and may potentially affect stability. This means that the rate of switching between the adaptive controllers has to be limited. In this paper, however, we do not explicitly limit the rate of switching.

Since the number of vehicles tracked may change in time, the commanded velocity vector also changes. Let $\lambda_1(t)$ and $\lambda_2(t)$ denote LOS angles with respect to the two closest vehicles, $\hat{\lambda}_1(t)$ and $\hat{\lambda}_2(t)$ the associated LOS unit vectors, and $\vec{V}_{FC_1}$ and $\vec{V}_{FC_2}$ the commanded velocity vectors for regulating range from the two closest vehicles. Then, the velocity vector command is given as

$$\begin{aligned} &If \quad NV = 1 \\ &\vec{V}_{cmd} = c_1\vec{V}_{OA} + (1-c_1)\left(\vec{V}_{nom} - k(1-c_1)\left\langle \vec{V}_{nom} \bullet \hat{\lambda}_1 \right\rangle \hat{\lambda}_1\right) + k(1-c_1)\vec{V}_{FC_1} \end{aligned} \tag{39}$$

$$\begin{aligned} &If \quad NV = 2 \\ &\vec{V}_{cmd} = c_1\vec{V}_{OA} + (1-c_1)\left(\vec{V}_{nom} - k(1-c_1)\left[\left\langle \vec{V}_{nom} \bullet \hat{\lambda}_1 \right\rangle \hat{\lambda}_1 + \left\langle \vec{V}_{nom} \bullet \hat{\lambda}_2 \right\rangle \hat{\lambda}_2\right]\right) + k(1-c_1)\left[\vec{V}_{FC_1} + \vec{V}_{FC_2}\right] \end{aligned} \tag{40}$$

$$\begin{aligned} &If \quad NV = 0 \\ &\vec{V}_{cmd} = c_1\vec{V}_{OA} + (1-c_1)\vec{V}_{nom} \end{aligned} \tag{41}$$

where $\langle \bullet \rangle$ is the dot product operator, and $k > 0$ is a tuning parameter that indicates the relative priority for formation control with respect to nominal velocity vector tracking.

Equations (39) and (40) are constructed with the objective that the velocity vectors should converge to $\vec{V}_{nom}$ when the commanded range errors are zero, $\vec{V}_{nom}$ is the same for all vehicles, and when there are no obstacles to avoid. This can be understood by noting that $\left\langle \vec{V}_{nom} \bullet \hat{\lambda}_1 \right\rangle \hat{\lambda}_1$ $\left[\left\langle \vec{V}_{nom} \bullet \hat{\lambda}_2 \right\rangle \hat{\lambda}_2\right]$ is the projection of $\vec{V}_{nom}$ along the unit vector direction $\hat{\lambda}_1$ $(\hat{\lambda}_2)$, and $\vec{V}_{FC_1}$ $(\vec{V}_{FC_2})$ is an estimate of the velocity of the closest (second closest) neighbor along $\hat{\lambda}_1$ $(\hat{\lambda}_2)$ when the commanded range errors are zero. So, the desired equilibrium configuration for the formation is not reached unless $\left\langle \vec{V}_{nom} \bullet \hat{\lambda}_1 \right\rangle \hat{\lambda}_1$ $\left[\left\langle \vec{V}_{nom} \bullet \hat{\lambda}_2 \right\rangle \hat{\lambda}_2\right]$ equals $\vec{V}_{FC_1}$ $(\vec{V}_{FC_2}) \Rightarrow \vec{V}_{cmd} = \vec{V}_{nom}$.

A. Simulation Results

The first set of results with the leaderless formation control scheme is shown for a group of 4 aircraft with identical nominal velocity vectors $\vec{V}_{nom}$.

The nominal velocity vector is a sinusoidal heading profile at constant speed

$$\begin{aligned} V_{nom} &= 1.5 \\ \psi_{nom} &= \sin\left(t/5\right) \end{aligned} \tag{39}$$

The value of R_{com} chosen is 0.5. The initial positions of the aircraft were chosen such that each aircraft was tracking 2 neighboring aircraft. Figure 11 shows the trajectory plot for the formation. Note that the dimensions along the x-axis have been scaled up in the plot below.

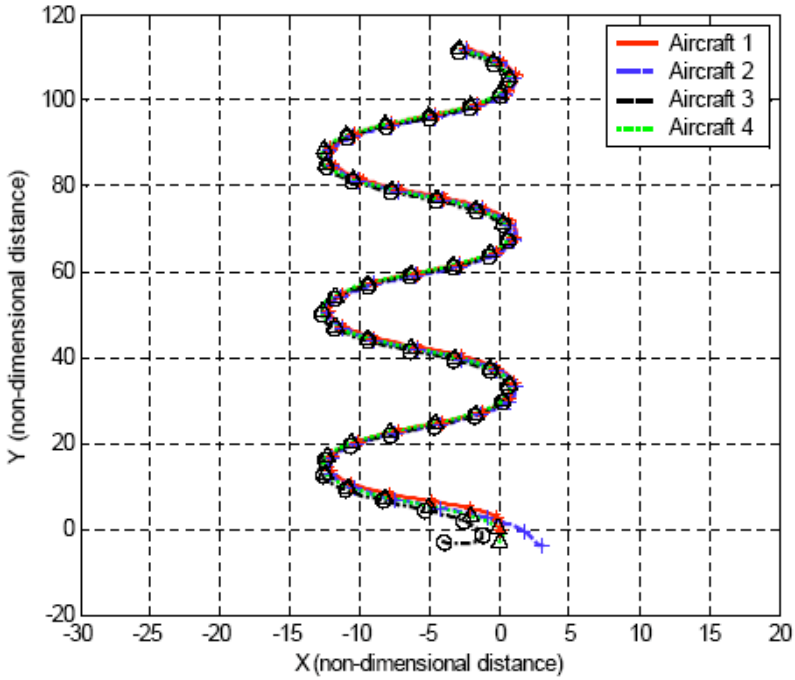

Fig. 11 Leaderless formation trajectory for identical nominal velocity

Figure 12 shows the LOS range histories for all aircraft in formation. The plot shows convergence to the commanded range R_{com} of the LOS ranges from the 2 closest neighbors for all aircraft. The plot also shows that aircraft 1 and 3 are separated by a range greater than R_{com} in steady-state (top-left and bottom-left subplots), and that aircraft 2 and 4 seem to be at the commanded range from all aircraft (top-right and bottom-right subplots). This suggests that the formation has split into 2 groups with aircrafts 2 and 4 common to both groups. The splitting of the formation is a common result with the leaderless formation control scheme.

Figure 13 shows the plot of some of the inversion errors Δ_{ij} plotted against the corresponding NN outputs $\nu_{ad_{(i,j)}}$. The plot shows very good tracking of the Δ_{ij}. Note in particular the first subplot. The signal $\nu_{ad(1,3)}$ is the NN output of aircraft 1 designed to track aircraft 3. From figure 12, we know that aircraft 1 does not regulate range from aircraft 3 because aircraft 2 and 4 are its closest neighbors. This shows that adaptation continues despite the adaptive control not being in control of the plant.

Next we consider a group of 5 aircraft tracking a sequence of waypoints in the counter-clockwise direction. The hyperlink multimedia 1 shows the dynamic trajectory of the formation. Waypoints are marked in the plot by red crosses. The plot shows that the formation is achieved and maintained at places where there are no obstacles. The formation is also seen to split to go around an obstacle and later rejoin.

Figure 14 shows the LOS ranges between all pairs of aircraft in the formation. It can again be concluded that the formation has split into groups by noting that only some of the LOS ranges have converged to the commanded value R_{com}.

Two large spikes are seen in the LOS range histories shown in Fig. 14. To understand the spikes, one must carefully view the dynamic trajectory of the formation (multimedia link 2). The spike in the variable R_{15} occurring between approximately 25-45 seconds is a consequence of aircraft 5 moving away from aircraft 1 while splitting around the first obstacle encountered after turning left past the first waypoint. Note that aircraft 2, 3, and 4 are not tracking either aircraft 1 or 5 during this interval because they are far behind them. A second large spike is seen between 90-100 seconds involving the range variables R_{12}, R_{23}, R_{24} and R_{25}. Seen together with the dynamic trajectory, it is clear that this large spike occurs when because aircraft 2 separates from the rest of the formation at the last obstacle the formation encounters.

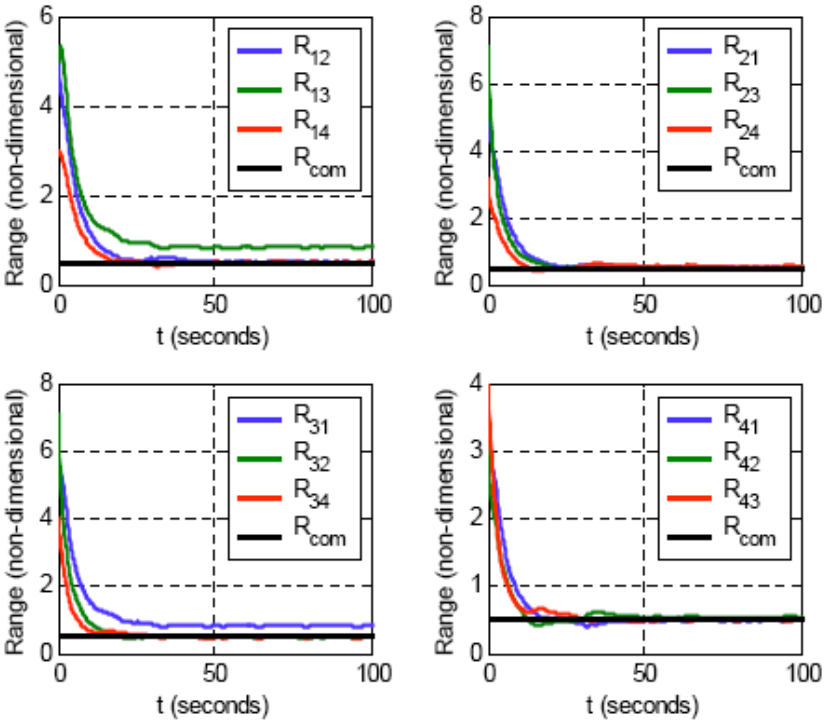

Fig. 12 LOS range histories for leaderless formation.

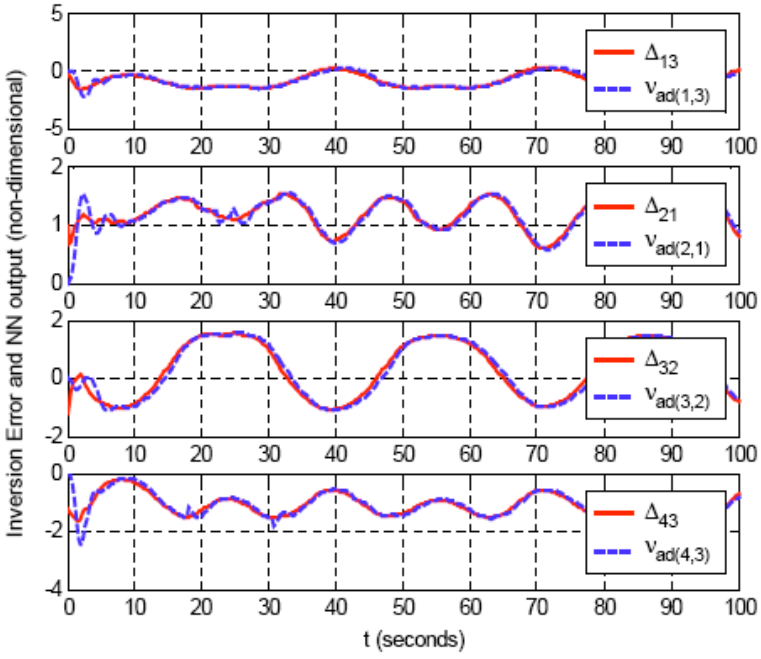

Fig. 13 Inversion error and NN outputs.

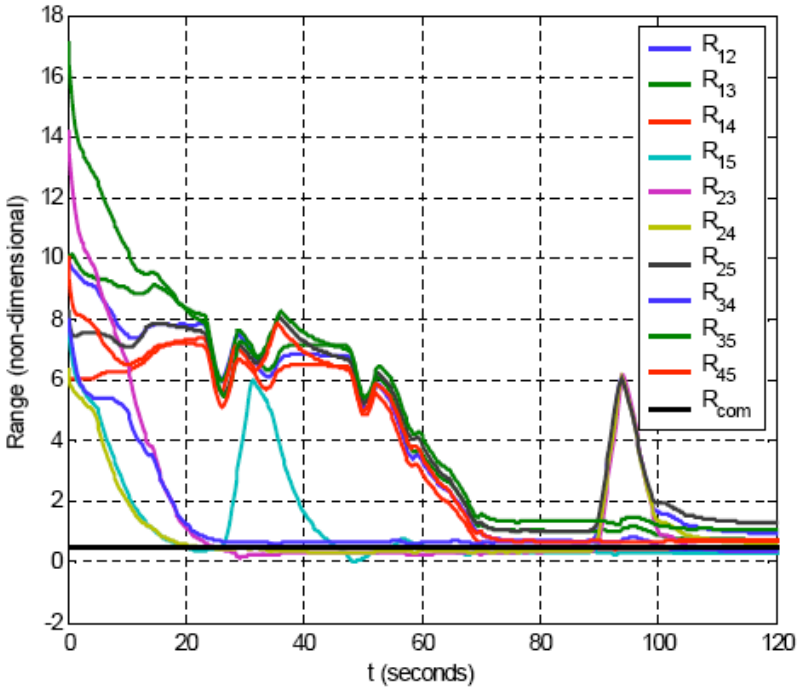

Fig. 14 LOS range histories for leaderless formations with waypoint tracking.

Figure 15 shows the number of vehicles being tracked by every vehicle during the maneuver. The number of neighboring vehicles tracked is seen to change in time.

The link in multimedia 2 shows a maneuver in which the formation changes from a wide formation to a line-shaped formation. Line-shaped formations are desirable when the formation is required to squeeze through narrow corridors. The line-shaped formation is achieved when each vehicle tracks the nearest vehicle that lies in a conical region in front of it. When there are no vehicles in this conical region, each vehicle has nominal motion directed towards a waypoint. This waypoint is common to all vehicles and can be considered to be a point at the entrance of the narrow corridor.

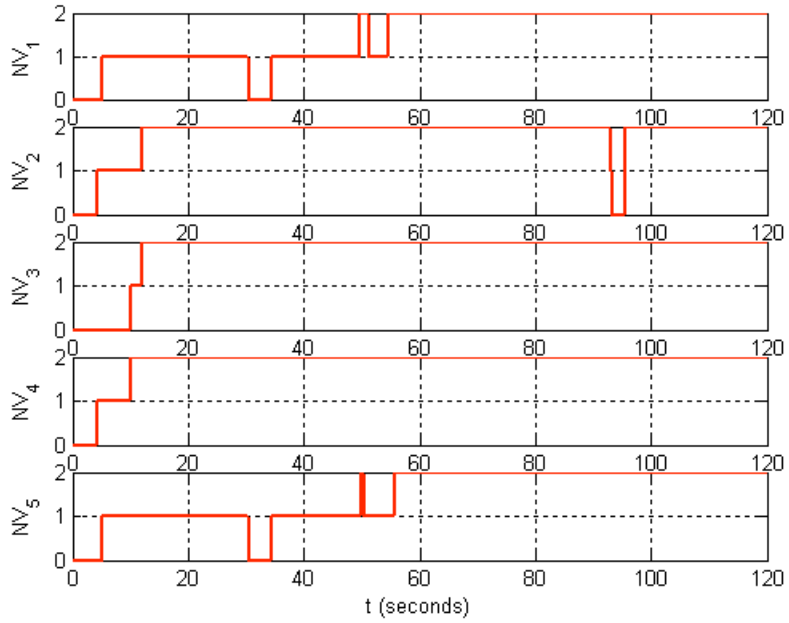

Fig. 15 Number of neighbor vehicles (*NV*) tracked.

There are a few drawbacks of the proposed approach. The first is the need for each aircraft in the formation to have the neighboring aircraft it is tracking to be within its field-of-view (FOV) at all times. Since each aircraft could be tracking multiple aircraft and FOVs could be small, this seems like a restrictive assumption. Consequently, to satisfy this assumption, the maneuvers of the aircraft in formation may have to be restricted. Secondly, visual data of neighboring aircraft is not available when they are obscured by obstacles. This loss of vision data is not presently accounted for in our approach. Finally, range is not a directly available measurement from the vision sensors. The range needs to be estimated from the true vision data and this is not a trivial problem [19,20,21]. Alternatively, we can directly regulate the angle subtended by the neighboring aircraft on the image plane in place of the range [22]. This subtended angle is a measurement directly available from the vision sensors that is roughly proportional to the size of the neighboring aircraft and inversely proportional to the range from the neighboring aircraft[19].

VI. Conclusions

We have formulated a decentralized adaptive guidance strategy that enables safe and coordinated motion of a group of unmanned vehicles in an environment with obstacles. We have shown that adaptation benefits by enhancing the cooperation between the vehicles in formation.

We have implemented two coordination schemes for formation control: leader-follower formation scheme and leaderless formation scheme. The leaderless formation control scheme is proposed as a way of dealing with the robustness issues of the leader-follower formation control scheme. The decentralized formations that result from the application of this scheme can perform maneuvers like splitting / rejoining around obstacles and changing into line-shaped formation in order to move through narrow corridors. Future work will involve testing of the adaptive guidance algorithms in a nonlinear 6 DOF simulation.

Acknowledgments

This research has been sponsored under AFOSR contract F4960-01-1-0024 and under NRTC contract NCC 2-945.

References

[1]Das, A. V., Fierro, R., Kumar, V., Ostrowski, J. P., Spletzer J., and Taylor, C. J., "A Vision-based Formation Control Framework," *IEEE Transactions on Robotics and Automation*, Vol. 18, No. 5, Oct. 2002, pp. 813-825.

[2]Sattigeri, R., Calise, A. J., and Evers, J., "An Adaptive Approach to Vision-based Formation Control," AIAA Paper 2003-5727*, AIAA Guidance, Navigation and Control Conference*, Aug. 2003.

[3]Beard, R. W., Lawton J., and Hadeagh, F. Y., "A Feedback Architecture for Formation Control," *Proceedings of the American Control Conference*, Vol. 6, June 2000, pp. 4087-4091.

[4]Leonard, N. E., and Fiorelli, E., "Virtual Leaders, Artificial Potentials and Coordinated Control of Groups," *IEEE Conference Decision and Control,* Dec. 2001, pp. 2968 - 2973.

[5]Balch, T., and Arkin, R. C., "Behavior-based Formation Control for Multi-robot Teams," *IEEE Transactions on Robotics and Automation*, Vol. 14, Nov 1998, pp. 926-934.

[6]Mataric, M., *Interaction and Intelligent Behavior*, PhD thesis, MIT, Electrical Engineering and Computer Science, 1994.

[7]Bonabeau, E., Dorigo, M., and Theraulaz, G., *Swarm Intelligence: From Natural to Artificial Systems,* Oxford Univ. Press, 1999.

[8]Reynolds, C. W., "Flocks, Herds and Schools: a Distributed Behavioral Model," *Computer Graphics*, Vol. 21, No. 4, pp. 71-87, 1987.

[9]Tanner, H. G., Jadbabaie, A., and Pappas, G. J., "Stable Flocking of Mobile Agents, Part I: Fixed Topology," *IEEE Conference on Decision and Control,* Dec. 2003, pp. 2010-2015.

[10]Olfati, S., and Murray, R. M., "Flocking with Obstacle Avoidance: Cooperation with Limited Communication in Mobile Networks," *Proceedings of the IEEE Conference on Decision and Control,* Hawaii, December 2003.

[11]Hovakimyan, N., and Calise, A.J., "Adaptive Output Feedback Control of Uncertain Multi-Input Multi-Output Systems Using Single Hidden Layer Networks," *International Journal of Control*, 2002.

[12]Johnson, E., and Calise, A.J., "Feedback Linearization with Neural Network Augmentation applied to X-33 Attitude Control," *AIAA-2000-4157 Guidance, Navigation and Control Conference*, Denver, CO, August 2000.

[13]Johnson, E., and Calise, A. J., "Neural Network Adaptive Control of Systems with Input Saturation," *Proceedings of the American Control Conference*, June 2001, pp. 3527-3532.

[14]Isidori, A., *Nonlinear Control Systems,* Springer Verlag, 1995.

[15]Calise, A.J., Hovakimyan, N., and Idan, M., "Adaptive Output Feedback Control of Nonlinear Systems using Neural Networks," *Automatica*, Vol. 37, No. 8, Aug. 2001.

[16]Hovakimyan, N., Lee, H., and Calise, A. J., "On Approximate NN Realization of an Unknown Dynamic System from its Input-Output History," *Proceedings of the American Control Conference*, June 2000, pp. 919-923.

[17]Lavretsky, E., Hovakimyan, N., and Calise, A.J, "Upper Bounds for Approximation of Continuous-Time Dynamics Using Delayed Outputs and Feedforward Neural Networks," *IEEE Transactions on Automatic Control*, Vol. 8, Sept. 2003, pp.1606-1610.

[18]Idan, M., Johnson, M., and Calise, A. J., "A Hierarchical Approach to Adaptive Control for Improved Flight Safety," AIAA-2001-4209, *AIAA Guidance, Navigation and Control Conference*, Aug. 2001.

[19]Betser, A., Vela, P., and Tannenbaum, A., "Automatic Tracking of Flying Vehicles Using Geodesic Snakes and Kalman Filtering," Accepted for publication in *IEEE Conference on Decision and Control*, 2004.

[20]Watanabe, Y., Johnson, E. N., and Calise, A. J., "Optimal 3-D Guidance from a 2-D Vision Sensor," *AIAA Guidance, Navigation, and Control Conference,* Aug. 2004.

[21]Madyastha, V., and Calise, A. J., "An Adaptive Filtering Approach to Target Tracking," Submitted to *American Control Conference*, 2005.

[22]Johnson, E. N., Calise, A. J., Sattigeri, R., Watanabe, Y., Madyastha, V., "Approaches to Vision-Based Formation Control," Accepted for publication in *IEEE Conference on Decision and Control*, 2004.